

# An Enzyme Model Which Mimics Chymotrypsin and N-Terminal Hydrolases

José J. Garrido-González, M<sup>a</sup> Mercedes Iglesias Aparicio, Miguel Martínez García, Luis Simón, Francisca Sanz, Joaquín R. Morán,\* and Angel L. Fuentes de Arriba\*



Cite This: *ACS Catal.* 2020, 10, 11162–11170



Read Online

ACCESS |



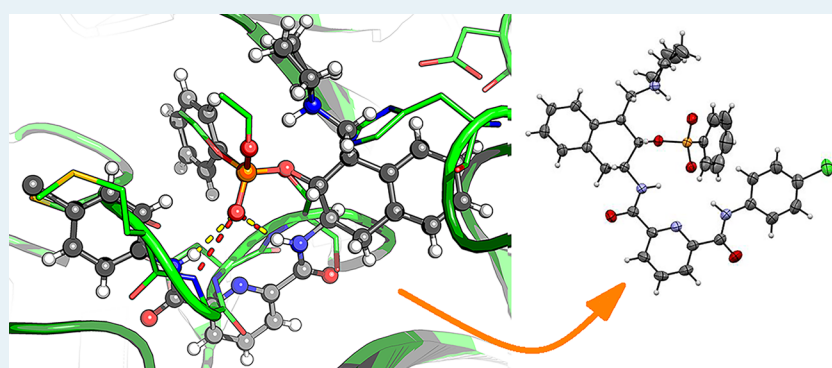
Metrics & More



Article Recommendations



Supporting Information



**ABSTRACT:** Enzymes are the most efficient and specific catalysts to date. Although they have been thoroughly studied for years, building a true enzyme mimic remains a challenging and necessary task. Here, we show how a three-dimensional geometry analysis of the key catalytic residues in natural hydrolases has been exploited to design and synthesize small-molecule artificial enzymes which mimic the active centers of chymotrypsin and N-terminal hydrolases. The optimized prototype catalyzes the methanolysis of the acyl enzyme mimic with a half-life of only 3.7 min at 20 °C, and it is also able to perform the transesterification of vinyl acetate at room temperature. DFT studies and X-ray diffraction analysis of the catalyst bound to a transition state analogue proves the similarity with the geometry of natural hydrolases.

**KEYWORDS:** artificial hydrolase, enzyme mimic, chymotrypsin, N-terminal hydrolase, organocatalysis, hydrogen bond, oxyanion hole, transesterification

## INTRODUCTION

Enzymes are the only catalysts that operate in biochemistry; however, they have also found important applications in industry since, to date, many processes cannot be carried out economically with synthetic catalysts.<sup>1</sup> The highly selective 11-hydroxylation of 11-deoxycortisol to yield cortisol by 11- $\beta$ -hydroxylase is a good example.<sup>2</sup>

In particular, hydrolytic enzymes, which are a family of more than 200 enzymes responsible for lipid, sugar, and peptide hydrolysis, have found important applications in fine chemical production, the food and detergent industry, paper manufacturing, chemical degradation processes, biomass conversion, and the pharma industry.<sup>3</sup> However, their low stability, high cost, and risk of denaturalization under extreme pH, temperature, or salt conditions make them tricky substances to work with. Hence, there is an increasing interest in developing artificial hydrolases for industrial, academic, and therapeutic purposes. Suh has recently outlined the importance of artificial proteases as new catalytic drugs<sup>4</sup> for amyloid diseases.<sup>5</sup>

Chemists have tried to mimic hydrolases for a long time. Especially remarkable are the contributions of Lehn in enantioselective thiolysis reactions<sup>6</sup> as well as those of Breslow<sup>7</sup> and Cram<sup>8</sup> in the hydrolysis of nitrophenyl esters, with reaction rate increases up to  $7.5 \times 10^5$  and  $10^{11}$ , respectively. While most of these enzyme models rely on the formation of inclusion complexes of activated esters inside cyclodextrins, cucurbiturils, cavitands, and other macrocycles,<sup>7,9</sup> artificial enzymes which try to mimic the geometry of the catalytic triad of serine or cysteine proteases are much scarcer. One of the reasons is their challenging synthesis: each of the reactive groups in the active site corresponds to different domains of the protein backbone chain and are only brought

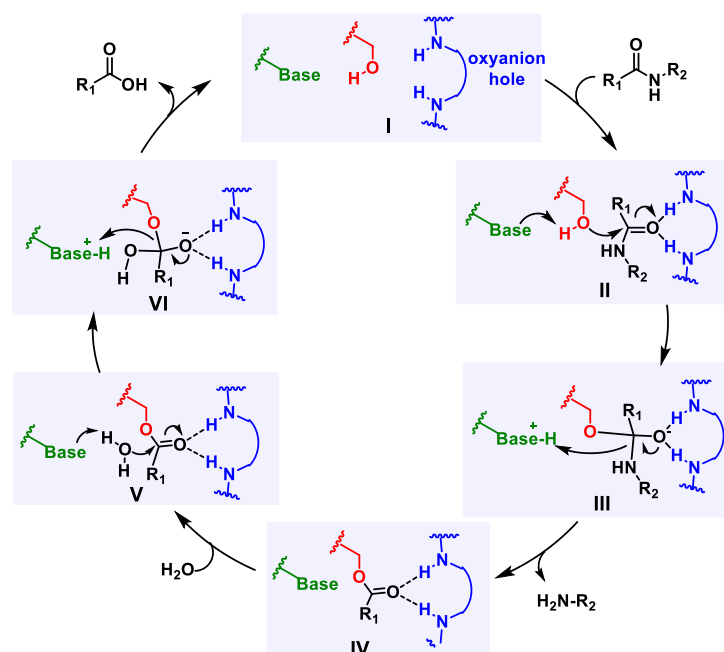
**Received:** May 13, 2020

**Revised:** August 13, 2020

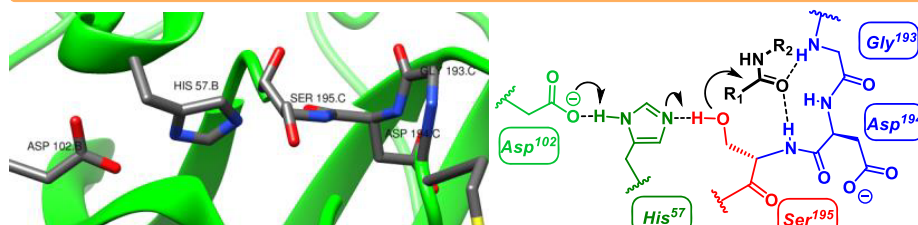
**Published:** August 31, 2020



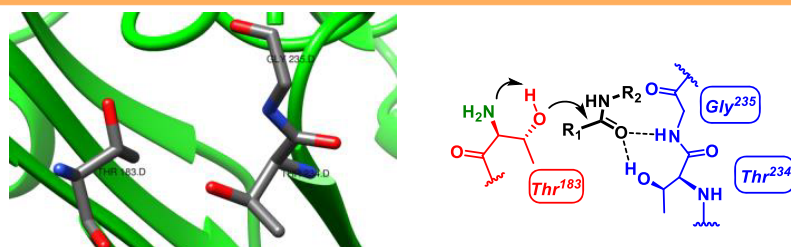
### A | Catalytic mechanism of hydrolytic enzymes



### B | Active center of bovine $\gamma$ -chymotrypsin



### C | Active center of human aspartylglucosaminidase



### D | This work - catalyst design

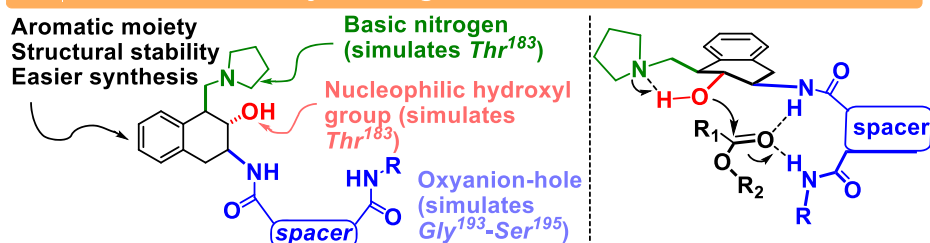


**Figure 1.** (A) General mechanism of hydrolytic enzymes. (B) Active center of bovine  $\gamma$ -chymotrypsin (PDB 1AB9). (C) Active center of human aspartylglucosaminidase (PDB 1APY). (D) Catalytic features of the hydrolase mimic designed in this work.

together when the protein folds in its tertiary structure (Figure 1B). Ema and Sakai<sup>10</sup> and Schafmeister<sup>11</sup> have reported small-molecule enzyme mimics able to simulate the catalytic triad of hydrolytic enzymes. Although large acceleration rates were

obtained, their systems are limited to highly activated vinyl trifluoroacetate esters. Several research groups have tried to mimic the three-dimensional arrangement of the catalytic groups in chymotrypsin by using polymer imprinting

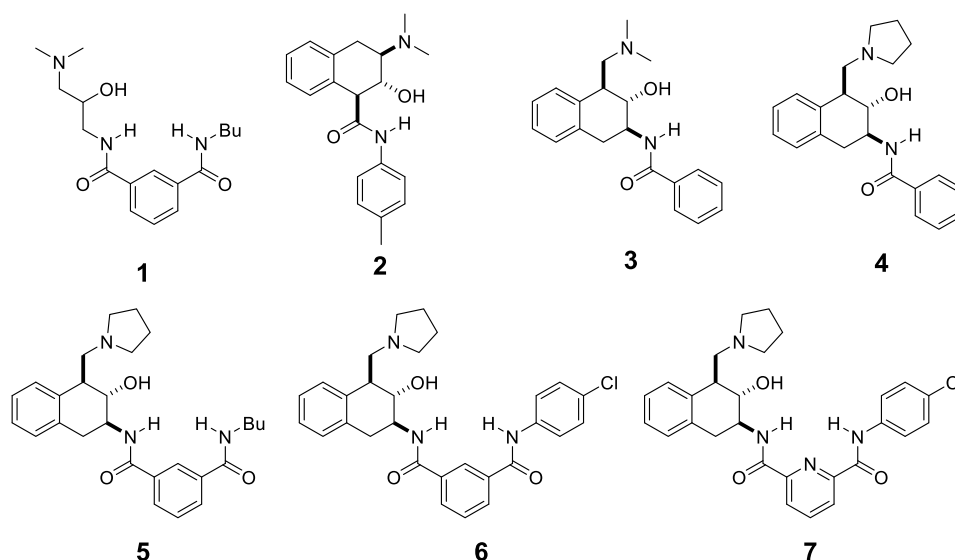


Figure 2. Hydrolase mimics synthesized in this work.

techniques<sup>12</sup> or by attaching the catalytic groups onto polymeric materials<sup>13</sup> or micelles;<sup>14</sup> however, the results are still not optimized enough to be applicable in industry. Connal has recently highlighted the state of the art of synthetic catalysts inspired by hydrolytic enzymes which is still far from reproducing reactions of native enzymes on esters, amides, and proteins under mild conditions.<sup>15</sup> In our opinion, a rational understanding of the geometry of the active center of hydrolytic enzymes, on the basis of an analysis of the X-ray structure of hydrolases, could be a promising starting point to design a true enzyme mimic. The synthesis and testing of small molecules which try to mimic the catalytic groups of the active center of hydrolases could shed some light on the importance of the geometry of the catalytic groups of the active site to achieve high levels of catalysis. Herein, we wish to report our findings.

Among all the different families of proteolytic enzymes, N-terminal hydrolases<sup>16</sup> are a superfamily of enzymes which lack the histidine–aspartate combination of the catalytic triad,<sup>17</sup> being replaced by a terminal  $-\text{NH}_2$  group which stems from a terminal serine, threonine, or cysteine (Figure 1C). This fact makes them attractive candidates for the development of artificial enzymes, since the combination of a simple 1,2-amino alcohol with a suitable oxyanion hole could provide a decent enzyme mimic. Although one would expect the amino group to be protonated in aqueous solution, the protein environment reduces the  $\text{pK}_a$  of the  $\alpha$ -amino group to a value close to histidine's first  $\text{pK}_a$  (6.2).<sup>18</sup> On the other hand, the usual hydrophobic pocket may not even be necessary, since chymotrypsin excludes water from the active center during its reactions.<sup>19</sup> According to Warshel, the main factor to explain enzymatic catalysis comes from a preorganized polar environment which is complementary with the guest transition state and which is mainly obtained through H bonds.<sup>20</sup> In fact, site-directed mutagenesis studies have shown that most of the catalytic activity of chymotrypsin ( $10^{10}$ ) can be explained with the H bonds of the oxyanion hole ( $10^4$ ) and the catalytic triad ( $10^6$ ).<sup>21</sup> Therefore, a similar array of H bonds from a small synthetic molecule may provide catalysis comparable to that of natural enzymes.

## RESULTS AND DISCUSSION

**Kinetic and Computational Studies.** Taking inspiration from natural chymotrypsin and N-terminal hydrolases, we synthesized enzyme mimic **1** (Figure 2, see the Supporting Information for its preparation). Catalyst **1** combines an oxyanion-hole mimic, based on an isophthalic acid moiety, a nucleophilic hydroxyl group, and a basic dimethylamine group. The isophthalic acid spacer, with two NHs and an aromatic C–H that can also behave as an H-bond donor, has been successfully used in the literature as an oxyanion-hole mimic.<sup>22</sup> The oxyanion hole and hydroxyl group are separated by two carbon atoms (as in the chymotrypsin catalytic triad; Figure 1B). Concurrently, we hope that the 1,2-amino alcohol moiety plays the same role as terminal threonine in N-terminal hydrolases, in which  $-\text{NH}_2$  and  $-\text{OH}$  groups are in a 1,2-disposition (Figure 1C). 1,2-Amino alcohols have already shown transacylation activity with activated esters.<sup>23</sup>

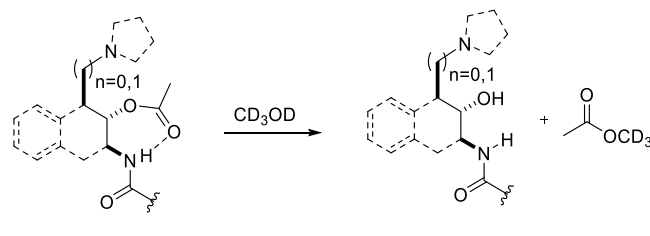
The classical mechanism of hydrolytic enzymes through the well-known catalytic triad requires an acylation step of a serine or cysteine residue ( $\text{II} \rightarrow \text{IV}$ , Figure 1A) and subsequent hydrolysis of the acyl intermediate by  $\text{H}_2\text{O}$  ( $\text{IV} \rightarrow \text{VI}$ , Figure 1A). It has been observed for both natural and artificial enzymes that the acylation step is faster than the acyl intermediate hydrolysis,<sup>10,23,24</sup> although these results may be biased, as most examples use activated esters as substrates, which possess a good leaving group that is not available for the second step. This difference in the reaction rates causes a lack of turnover,<sup>25</sup> as once the hydroxyl group of the enzyme mimic is acylated ( $\text{IV}$ , Figure 1A) it does not undergo further reaction.

To complement previous studies, we decided to tackle the *a priori*, more challenging acyl intermediate hydrolysis with enzyme mimic **1** (Figure 2). Hence, by aiming at the rate-limiting step of the mechanism, we should have a fast estimation of the possibilities of this scaffold to be used in hydrolysis or transesterification reactions. To test the catalytic activity of compound **1**, acetylation of its hydroxyl group was first performed in  $\text{Ac}_2\text{O}$ , and after isolation of acetylated catalyst **1**, it was transferred to an NMR tube and dissolved in deuterated methanol. Catalyst **1** was designed to be soluble in chloroform, which is a solvent that can mimic the hydrophobic

environment of the hydrolase active site. However, to speed up and simplify the study, as pseudo-first-order kinetics can be applied, deuterated methanol was used as the solvent and the deacetylation kinetics were followed by  $^1\text{H}$  NMR at 20  $^\circ\text{C}$ .

According to kinetic experiments (see the [Supporting Information](#)), deacetylation of **1a** by  $\text{CD}_3\text{OD}$  took place with a half-life of 187 min ([Table 1](#), entry 1). This result was slower

**Table 1. Half-Life (min) of the Methanolysis Reaction of Acetylated Catalysts 1a–7a**



entry	catalyst	$t_{1/2}$ (min) <sup>a</sup>
1	1a	187
2	2a	165
3	3a	87
4	4a	17
5	5a	12
6	6a	15
7	7a	3.7

<sup>a</sup>Ca. 10 mg of the acetylated catalyst **1a–7a** was dissolved in 400  $\mu\text{L}$  of  $\text{CD}_3\text{OD}$ , and  $^1\text{H}$  NMR spectra were recorded periodically at 20  $^\circ\text{C}$ . The half-life was determined by  $^1\text{H}$  NMR integration.

than expected, as the biological conversion of ethyl acetate to ethanol takes place in only 5–10 min.<sup>26</sup> Probably, the free rotation of the methylene groups generates nonproductive conformations in the catalyst structure due to the establishment of intramolecular H bonds between the basic dimethylamine nitrogen and the oxyanion hole, which hamper catalyst activity.

Although Breslow and others have shown that more structural flexibility provided improved outcomes in enzyme mimics,<sup>27</sup> in this case it is necessary to anchor the different catalytic groups to a rigid scaffold in order to prevent nonproductive conformations. This is a challenging task, because if the distances between the different groups are not appropriate, the catalyst will not show any catalytic activity. After screening different possibilities, we chose a rigid template based on a dihydronaphthalene scaffold to anchor the basic group, nucleophilic hydroxyl group, and oxyanion-hole moiety ([Figure 1D](#)). The presence of the aromatic ring confers structural stability to the molecule and facilitates the synthesis.

With these premises in hand, catalyst **2** was prepared. For the sake of synthetic simplicity, the oxyanion-hole role was performed by a single NH. Under these conditions, a small reduction in the half-life of 20 min was observed in comparison with catalyst **1** ([Table 1](#), entry 2).

Looking for alternative scaffolds, we envisaged a 1,3-amino alcohol geometry. Although this disposition differs from the 1,2-amino alcohol scaffold in N-terminal hydrolases, water molecules could be necessary in N-terminal hydrolases to transport the proton between  $-\text{NH}_2$  and  $-\text{OH}$  groups, preventing in this way the formation of a strained four-membered ring.<sup>28</sup> The greater distance between the hydroxyl

and amino groups in a 1,3-amino alcohol arrangement could be a key aspect to circumvent this problem. An extensive conformational search for a model compound (see the [Supporting Information](#)) suggested that the equatorial disposition of all the catalytic groups, required to make the proton transport feasible, is the most stable conformation by more than 4.6 kcal/mol over the most stable axial disposition ([Figure 3](#)). This geometry provides a distance of 2.75 Å

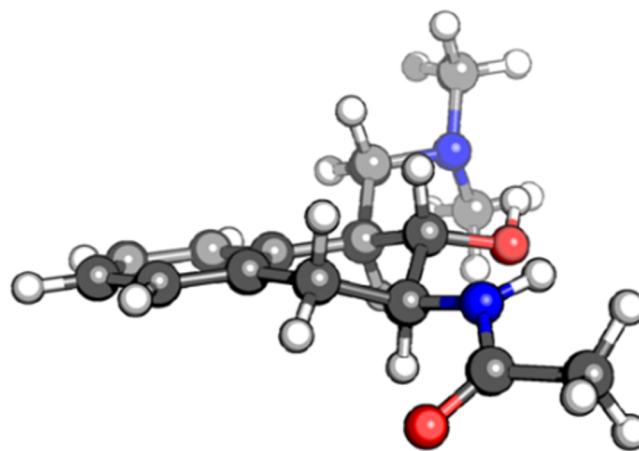


**Figure 3.** Most stable conformation of a model of catalysts **3–7** showing the equatorial arrangement of catalytic groups.

between OH and  $\text{NH}_2$ , which is close to the 2.92 Å between the same groups in N-terminal hydrolase human aspartylglucosaminidase or the 3.02 Å between OH and imidazole in bovine  $\gamma$ -chymotrypsin. In this enzyme one of the NHs in the oxyanion hole is 3.09 Å from the serine OH, while in the model of [Figure 3](#) this distance is around 2.66 Å.

Thus, this motif was incorporated in catalyst **3**. Pleasingly, kinetic studies showed that the catalyst **3** skeleton is almost twice as good as that of catalyst **2**, with a half-life of 87 min ([Table 1](#), entry 3).

Next, a series of modifications were introduced in the catalyst **3** structure to improve its catalytic activity. While the replacement of the dimethylamino group for a more basic pyrrolidine entailed a 5-fold decrease in half-life ([Table 1](#), entry 4), the introduction of a second NH group via an isophthalic acid moiety to construct the oxyanion-hole motif allowed reducing the half-life to 12 min ([Table 1](#), entry 5).

To our surprise, increasing the acidity of the second NH in the oxyanion hole of catalyst **6** did not reduce the reaction rate ([Table 1](#), entry 6). Probably the rigidity of the dihydronaphthalene scaffold prevents the formation of the required short H bond between the acetate carbonyl group and the aromatic isophthalic NH, favoring the formation of some kind of dimer. Indeed, the  $^1\text{H}$  NMR spectrum of **6a** showed a shielding of 0.4 ppm for the isophthalic NH in comparison with the same NH in free catalyst **6** ([Figure 4](#)).

To shorten the distance between this NH bond and the carbonyl group, an oxyanion-hole mimic with a shorter distance between both NHs was explored. In this regard, 2,6-pyridinedicarboxylic acid may be a reasonable choice, since aromatic C–N distances (1.33 Å) are shorter than aromatic C–C distances (1.39 Å), the pyridine nitrogen nonbonding lone pair should direct the NHs toward the cavity,<sup>29</sup> and also the pyridine ring should enhance the NH acidity. According to our expectations, catalyst **7** showed a stronger intramolecular

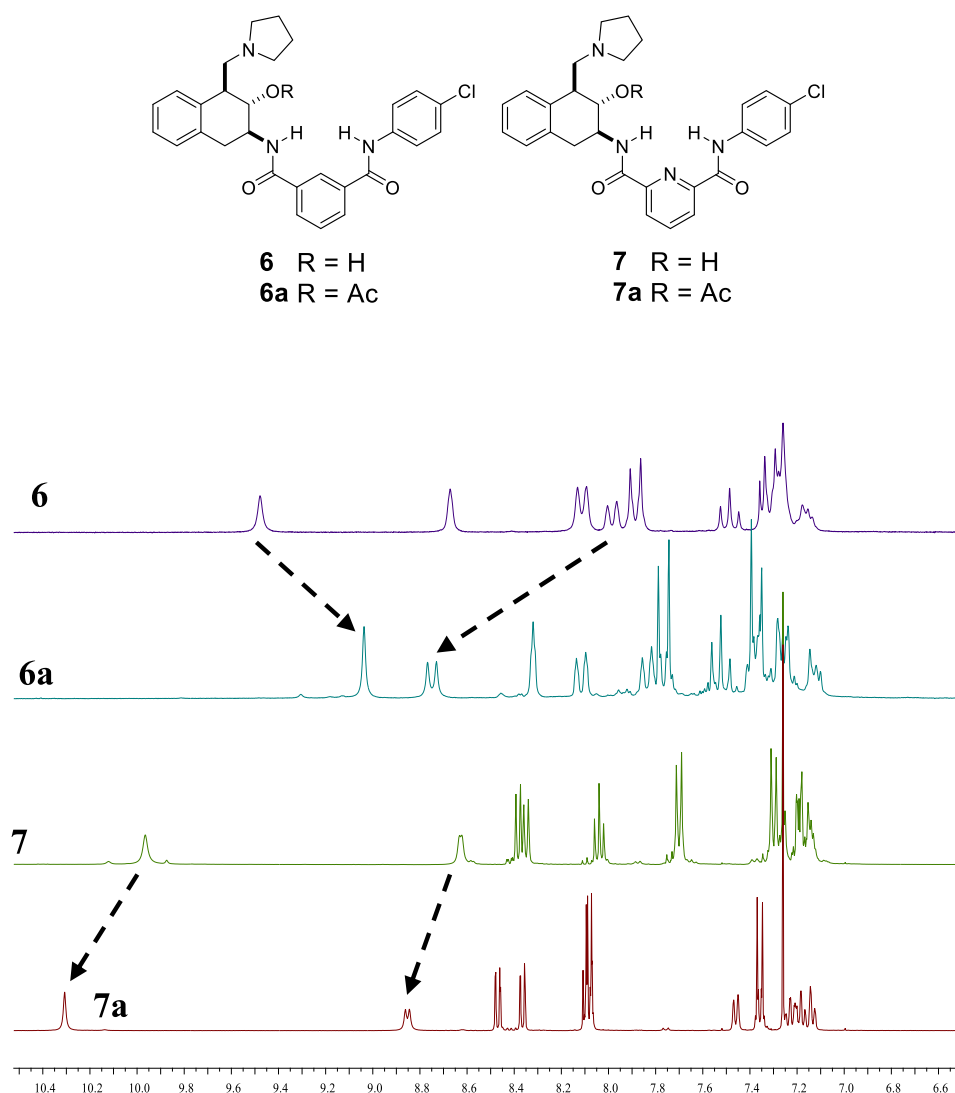


**Figure 4.**  $^1\text{H}$  NMR spectra (6.6–10.4 ppm) showing the movement of NH signals of catalysts **6** and **7** after acetylation.

H bond between the acetate carbonyl group and the aromatic NH, which was deshielded by 0.34 ppm in the presence of the acetate group (Figure 4).

DFT studies of the reaction transition state supported this observation, showing a short H bond of 2.8 Å between the isophthalic NH and the carbonyl oxygen atom (Figure 5).

Kinetics studies corroborated this hypothesis, as the methanolysis of **7a** showed a half-life of only 3.7 min (Table 1, entry 7). Figure 6 collects the variation with time of the molar fraction of the acetylated catalysts **1–7** prepared in this study.

**Transesterifications and Association Studies.** Encouraged by this result, we next tested the ability of compound **7** to catalyze the transesterification of vinyl acetate. Interestingly, low catalyst loadings of **7** (<1 mol %) were enough to catalyze the transesterification between vinyl acetate and methanol with 50% conversion after 68 h at 20 °C (Figure 7). No reaction took place in the absence of catalyst after 100 h. Also, compound **7a** could be obtained after 3 days by mixing catalyst **7** in vinyl acetate, showing the participation of the acyl intermediate in the reaction mechanism. To our knowledge this is the first time that a small-molecule hydrolase mimic has been able to catalyze the transesterification of vinyl acetate.

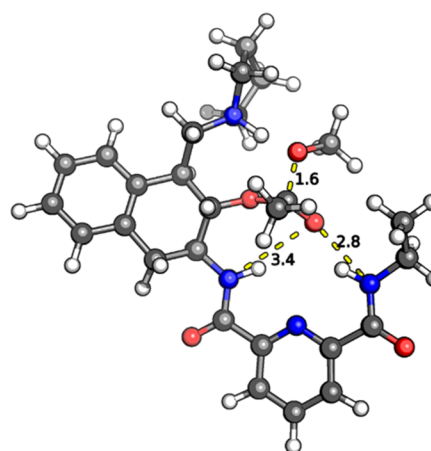


**Figure 5.** Calculated geometry of the transition state structure for the methanolysis reaction of compound **7a**. Selected distances between heteroatoms are depicted in angstroms.

Next, to prove the enzyme-like similarities of compound **7**, the association constant between catalyst **7** and EtOAc was measured by  $^1\text{H}$  NMR titration in  $\text{CDCl}_3$  at 20 °C. Successive



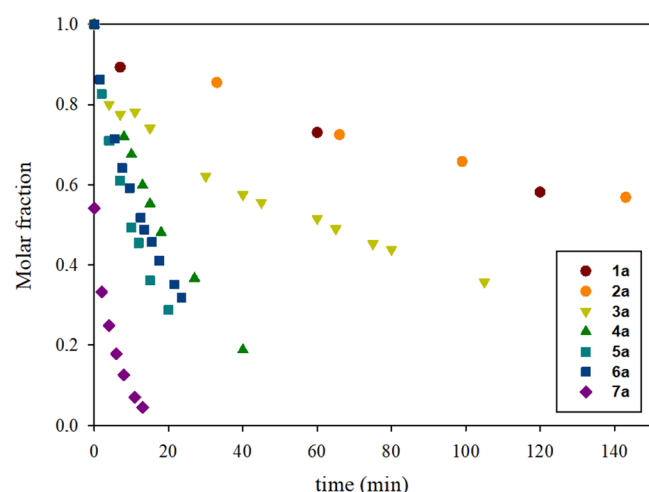
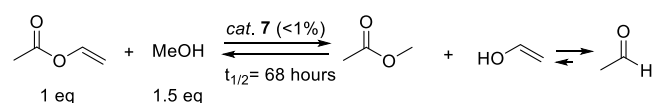


**Figure 6.** Time-dependent methanolysis of acetylated catalysts 1–7.



Proposed mechanism:

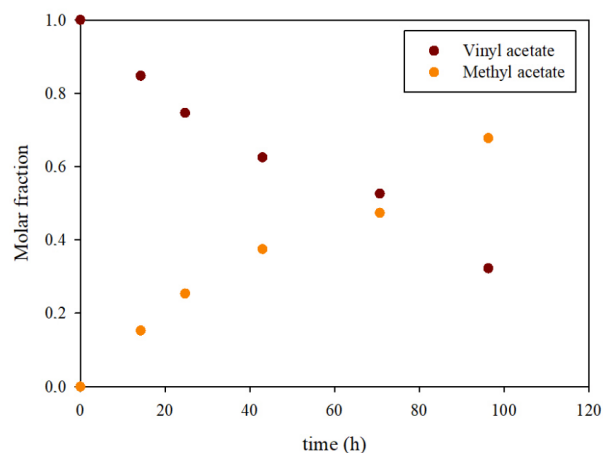
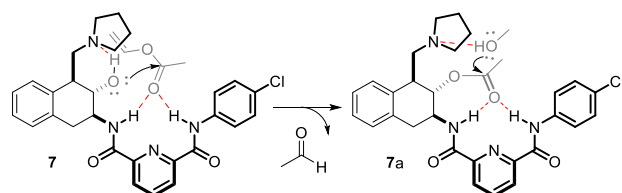


**Figure 7.** Time-dependent transesterification of vinyl acetate catalyzed with compound 7.

additions of ethyl acetate aliquots to a solution of catalyst 7 in  $\text{CDCl}_3$  and plotting of the signal shifts vs equivalents of ethyl acetate gave an association constant of  $0.79 \text{ M}^{-1}$  (see the [Supporting Information](#)). This value could explain the still low reaction rate for transesterification reactions in comparison with deacetylation reactions.

**X-ray Studies.** In order to show that catalyst 7 possesses a well-preorganized polar environment complementary to the transition state, its reaction with the transition state mimic phenylphosphonic acid chloride was performed ([Figure 8A](#)). Pleasingly, X-ray-quality crystals of the product were obtained

from slow evaporation of a dichloromethane/methanol solution.

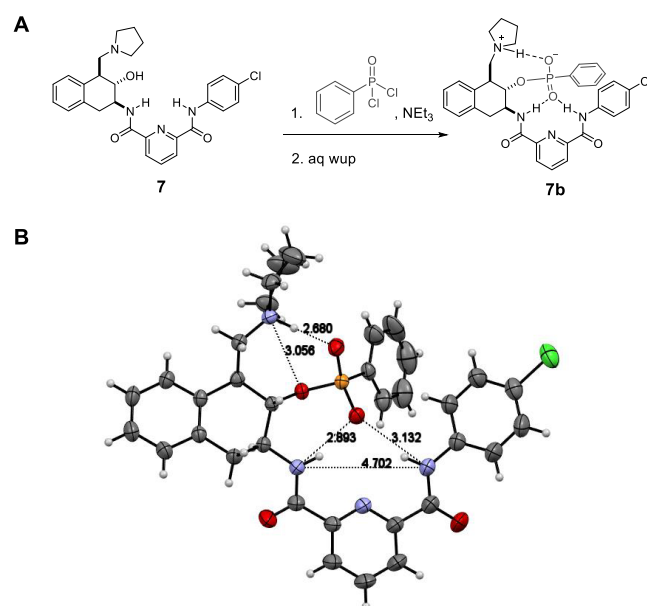


**Figure 8.** (A) Reaction of compound 7 with phenylphosphonic acid chloride. (B) X-ray diffraction structure of compound 7b. Selected distances between heteroatoms are depicted in angstroms.

The single-crystal X-ray diffraction analysis showed a perfect fit of the phosphonate group inside the catalyst 7 oxanion hole ([Figure 8B](#)). The phosphoryl oxygen which mimics the negatively charged oxygen of the transition state establishes two H bonds of 2.89 and 3.13 Å with the pyridine aliphatic and aromatic NHs, respectively. The pyridine oxanion hole showed a 4.70 Å distance between both NHs, which is in good agreement with natural oxanion holes.<sup>30</sup>

The shortest H bond of only 2.68 Å is set between the pyrrolidinium group and one of the phosphate oxygen atoms. Both phosphoryl oxygens showed similar O–P distances of 1.49–1.50 Å, which can be explained by a negatively charged phosphonate group, which contributes to the short pyrrolidinium H bond.

One of the most attractive features of the structure is the similar distances established between the pyrrolidinium group with both the phosphonoester oxygen (3.06 Å) and the phosphoryl oxygen (2.68 Å), which may be a key factor in transporting the proton from the nucleophile to the leaving group.

The conclusions obtained from the X-ray structure of compound 7b agree with the observations detected in solution by  $^1\text{H}$  NMR, which revealed the deshielding of the oxanion-hole NHs upon acetylation of the catalysts. This implies that the acetate carbonyl group is hydrogen-bonded by the oxanion-hole NHs in a way similar to that for the phosphonate group which mimics the transition state of the reaction.

**Comparison with Natural Chymotrypsin.** To prove the similarity of catalyst 7 with the active site of a natural hydrolase, the single-crystal X-ray diffraction structure of compound 7b was superimposed with the active center of a chymotrypsin phosphate (PDB 1GCD) ([Figure 9](#)). The phosphate group was fixed for both compounds, which allowed

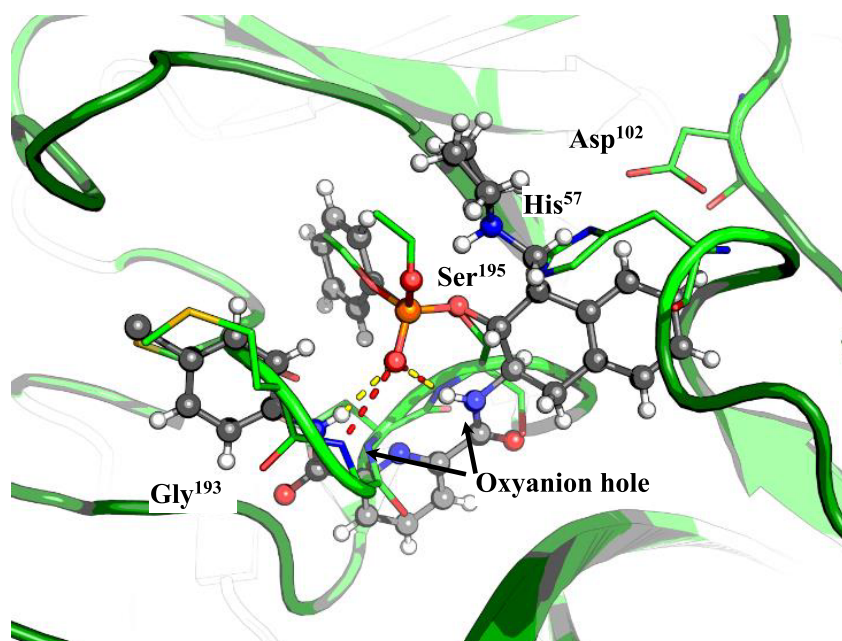


**Figure 9.** Superimposition of the crystal structure of chymotrypsin phosphate (ribbon model) and compound **7b** (ball and stick model), in which the phosphate group is fixed for both compounds. Hydrogen bonds between the oxyanion-hole NHs and the phosphate oxygen are depicted as red dashed lines for chymotrypsin phosphate and yellow dashed lines for compound **7b**.

a comparison of the geometry of the catalytic groups in the synthetic catalyst and the enzyme.

As can be observed in Figure 9, the geometry of compound **7b** is fairly similar to that of the active center of chymotrypsin, with the exception of the basic group, probably because the chymotrypsin phosphate is a neutral compound, which prevents the proximity of the imidazole ring due to the lack of hydrogen bonding, while in compound **7b** a strong H bond is set between pyrrolidinium and phosphate groups. A better fit is obtained for the oxyanion hole, with 2.90 Å distance between the phosphoryl oxygen and both the NH of Ser<sup>195</sup> and the NH of catalyst **7**. The second H bond of the oxyanion hole between Gly<sup>193</sup> and the phosphoryl oxygen is slightly shorter in chymotrypsin. The rigid pyridinedicarboxamide spacer, with a 4.70 Å distance between both NHs, is probably responsible for this fact, since in chymotrypsin, the oxyanion-hole distance between the NHs is around 4.30 Å.

## CONCLUSIONS

In conclusion, a detailed analysis of the key amino acid residues responsible for catalysis in serine proteases and N-terminal hydrolases has allowed us to simulate their active center by using a rigid cyclohexane skeleton where the base, nucleophilic hydroxyl group, and oxyanion hole have been rationally positioned. This small-molecule artificial enzyme catalyzes the deacetylation of enzyme mimics in less than 10 min and the transesterification of vinyl acetate at room temperature. Investigations to extend this reactivity to peptide bonds is currently ongoing in our laboratory and will be reported in due course.

## ASSOCIATED CONTENT

### Supporting Information

The Supporting Information is available free of charge at <https://pubs.acs.org/doi/10.1021/acscatal.0c02121>.

Experimental procedures, spectroscopic data, NMR titrations, kinetic data, ORTEP diagrams, X-ray crystal structure data, and modeling studies (PDF)

Crystallographic data (CIF)

### Accession Codes

CCDC 2031919 contains the supplementary crystallographic data for this paper. These data can be obtained free of charge via [www.ccdc.cam.ac.uk/data\\_request/cif](http://www.ccdc.cam.ac.uk/data_request/cif), or by emailing [data\\_request@ccdc.cam.ac.uk](mailto:data_request@ccdc.cam.ac.uk), or by contacting The Cambridge Crystallographic Data Centre, 12 Union Road, Cambridge CB2 1EZ, UK; fax: +44 1223 336033.

## AUTHOR INFORMATION

### Corresponding Authors

Joaquín R. Morán — Organic Chemistry Department, University of Salamanca, Salamanca E-37008, Spain; Email: [romoran@usal.es](mailto:romoran@usal.es)

Ángel L. Fuentes de Arriba — Organic Chemistry Department, University of Salamanca, Salamanca E-37008, Spain; [orcid.org/0000-0001-7424-8146](https://orcid.org/0000-0001-7424-8146); Email: [angelfuentes@usal.es](mailto:angelfuentes@usal.es)

### Authors

José J. Garrido-González — Organic Chemistry Department, University of Salamanca, Salamanca E-37008, Spain

M<sup>a</sup> Mercedes Iglesias Aparicio — Organic Chemistry Department, University of Salamanca, Salamanca E-37008, Spain

Miguel Martínez García — Organic Chemistry Department, University of Salamanca, Salamanca E-37008, Spain

Luis Simón — Chemical Engineering Department, University of Salamanca, Salamanca E-37008, Spain; [orcid.org/0000-0002-3781-0803](https://orcid.org/0000-0002-3781-0803)

Francisca Sanz — X-Ray Diffraction Service, University of Salamanca, Salamanca E-37008, Spain

Complete contact information is available at:

<https://pubs.acs.org/10.1021/acscatal.0c02121>

## Author Contributions

The manuscript was written through contributions of all authors. All authors have given approval to the final version of the manuscript.

## Notes

The authors declare no competing financial interest.

## ACKNOWLEDGMENTS

This work was supported by Junta de Castilla y León (European Regional Development Fund-SA069P17), the University of Salamanca (Own Research Programs-KCEP/463AC01), MINECO (CTQ2017-87529-R), and Fundación Memoria de D. Samuel Solórzano Barruso (FS/8-2019). J.J.G.-G. and A.L.F.d.A. gratefully acknowledge the University of Salamanca for predoctoral and postdoctoral fellowships, respectively. We also thank the NUCLEUS platform at University of Salamanca, A. López García and J. A. González Ramos for IT support, V. Obregón from Bio-Oils Huelva, and the University of Salamanca server housing service.

## DEDICATION

This article is dedicated to Professor Josefa Anaya on occasion of her retirement.

## REFERENCES

- (1) (a) Drauz, K.; Gröger, H.; May, O. *Enzyme Catalysis in Organic Synthesis*, 3rd ed.; Wiley-VCH: Weinheim, Germany, 2012; p 3. (b) Kirk, O.; Borchert, T. V.; Fuglsang, C. C. Industrial Enzyme Applications. *Curr. Opin. Biotechnol.* **2002**, *13*, 345–351.
- (2) Slater, L. B. Industry and Academy: The Synthesis of Steroids. *Hist. Stud. Phys. Biol. Sci.* **2000**, *30*, 443–480.
- (3) Chapman, J.; Ismail, A. E.; Dinu, C. Z. Industrial Applications of Enzymes: Recent Advances, Techniques, and Outlooks. *Catalysts* **2018**, *8*, 238–264.
- (4) Lee, T. Y.; Suh, J. Target-selective peptide-cleaving catalysts as a new paradigm in drug design. *Chem. Soc. Rev.* **2009**, *38*, 1949–1957.
- (5) (a) Suh, J. Progress in Designing Artificial Proteases: A New Therapeutic Option for Amyloid Diseases. *Asian J. Org. Chem.* **2014**, *3*, 18–32. (b) Lee, T. Y.; Suh, J. *Pure Appl. Chem.* **2009**, *81*, 255–262.
- (6) Lehn, J.; Sirlin, C. Molecular Catalysis: Enhanced Rates of Thiolysis with High Structural and Chiral Recognition in Complexes of a Reactive Macrocyclic Receptor Molecule. *J. Chem. Soc., Chem. Commun.* **1978**, 949–951.
- (7) (a) Breslow, R.; Dong, S. D. Biomimetic Reactions Catalyzed by Cyclodextrins and Their Derivatives. *Chem. Rev.* **1998**, *98*, 1997–2011. (b) Trainor, G. L.; Breslow, R. High Acylation Rates and Enantioselectivity with Cyclodextrin Complexes of Rigid Substrates. *J. Am. Chem. Soc.* **1981**, *103*, 154–158. (c) Breslow, R.; Trainor, G.; Ueno, A. Optimization of Metallocene Substrates for 1-Cyclodextrin Reactions. *J. Am. Chem. Soc.* **1983**, *105*, 2739–2744.
- (8) (a) Cram, D. J. The Design of Molecular Hosts, Guests, and Their Complexes. *Angew. Chem., Int. Ed. Engl.* **1988**, *27*, 1009–1020. (b) Cram, D. J.; Katz, H. E. An Incremental Approach to Hosts That Mimic Serine Proteases. *J. Am. Chem. Soc.* **1983**, *105*, 135–137. (c) Cram, D. J.; Lam, P. Y.-S.; Ho, S. P. Synthesis of a Partial Transacylase Mimic. *Ann. N. Y. Acad. Sci.* **1986**, *471*, 22–40. (d) Cram, D. J.; Katz, H. E.; Dicker, I. B. Host-Guest Complexation. 31. A Transacylase Partial Mimic. *J. Am. Chem. Soc.* **1984**, *106*, 4987–5000.
- (9) (a) Yuan, D. Q.; Kitagawa, Y.; Aoyama, K.; Douke, T.; Fukudome, M.; Fujita, K. Imidazolyl Cyclodextrins: Artificial Serine Proteases Enabling Regiospecific Reactions. *Angew. Chem., Int. Ed.* **2007**, *46*, 5024–5027. (b) Jiang, L.; Liu, Z.; Liang, Z.; Gao, Y. An Artificial Aspartic Proteinase System. *Bioorg. Med. Chem.* **2005**, *13*, 3673–3680. (c) Tabushi, I. Cyclodextrin Catalysis as a Model for Enzyme Action. *Acc. Chem. Res.* **1982**, *15*, 66–72. (d) Klöck, C.; Dsouza, R. N.; Nau, W. M. Cucurbituril-Mediated Supramolecular Acid Catalysis. *Org. Lett.* **2009**, *11*, 2595–2598. (e) Purse, B. W.; Rebek, J. Functional Cavitands: Chemical Reactivity in Structured Environments. *Proc. Natl. Acad. Sci. U. S. A.* **2005**, *102*, 10777–10782. (f) Soberats, B.; Sanna, E.; Martorell, G.; Rotger, C.; Costa, A. Programmed Enzyme-Mimic Hydrolysis of a Choline Carbonate by a Metal-Free 2-Aminobenzimidazole-Based Cavitand. *Org. Lett.* **2014**, *16*, 840–843.
- (10) Ema, T.; Tanida, D.; Matsukawa, T.; Sakai, T. Biomimetic Trifunctional Organocatalyst Showing a Great Acceleration for the Transesterification Between Vinyl Ester and Alcohol. *Chem. Commun.* **2008**, 957–959.
- (11) Kheirabadi, M.; Çelebi-Ölçüm, N.; Parker, M. F. L.; Zhao, Q.; Kiss, G.; Houk, K. N.; Schafmeister, C. E. Spiroligolyzymes for Transesterifications: Design and Relationship of Structure to Activity. *J. Am. Chem. Soc.* **2012**, *134*, 18345–18353.
- (12) (a) Chen, L.; Xu, S.; Li, J. Recent Advances in Molecular Imprinting Technology: Current Status, Challenges and Highlighted Applications. *Chem. Soc. Rev.* **2011**, *40*, 2922–2942. (b) Li, S.; Turner, A. P. F. *Molecularly Imprinted Catalysts: Principles, Syntheses, and Applications*; Elsevier: Amsterdam, 2015; pp 34–41. (c) Wulff, G. Enzyme-Like Catalysis by Molecularly Imprinted Polymers. *Chem. Rev.* **2002**, *102*, 1–28. (d) Chen, L.; Wang, X.; Lu, W.; Wu, X.; Li, J. Molecular Imprinting: Perspectives and Applications. *Chem. Soc. Rev.* **2016**, *45*, 2137–2111. (e) Mathew, D.; Thomas, B.; Devaky, K. S. Biomimetic Recognition and Peptidase Activities of Transition State Analogue Imprinted Chymotrypsin Mimics. *React. Funct. Polym.* **2018**, *124*, 121–128.
- (13) (a) Nothling, M. D.; Ganesan, A.; Condić-Jurkic, K.; Pressly, E.; Davalos, A.; Gotrik, M. R.; Xiao, Z.; Khoshdel, E.; Hawker, C. J.; O'Mara, M. L.; Coote, M. L.; Connal, L. A. Simple Design of an Enzyme-Inspired Supported Catalyst Based on a Catalytic Triad. *Chem.* **2017**, *2*, 732–745. (b) Delort, E.; Darbre, T.; Reymond, J.-L. A Strong Positive Dendritic Effect in a Peptide Dendrimer-Catalyzed Ester Hydrolysis Reaction. *J. Am. Chem. Soc.* **2004**, *126*, 15642–15643. (c) Uhlich, N. A.; Darbre, T.; Reymond, J.-L. Peptide Dendrimer Enzyme Models for ester hydrolysis and Aldolization Prepared by Convergent Thioether Ligation. *Org. Biomol. Chem.* **2011**, *9*, 7071–7084. (d) Maillard, N.; Biswas, R.; Darbre, T.; Reymond, J.-L. Combinatorial discovery of Peptide Dendrimer Enzyme Models Hydrolyzing Isobutyryl Fluorescein. *ACS Comb. Sci.* **2011**, *13*, 310–320. (e) Javor, S.; Reymond, J. L. Molecular dynamics and docking studies of single site esterase peptide dendrimers. *J. Org. Chem.* **2009**, *74*, 3665–3674. (f) Clouet, A.; Darbre, T.; Reymond, J. L. Esterolytic peptide dendrimers with a hydrophobic core and catalytic residues at the surface. *Adv. Synth. Catal.* **2004**, *346*, 1195–1204.
- (14) (a) Nothling, M. D.; Xiao, Z.; Hill, N. S.; Blyth, M. T.; Bhaskaran, A.; Sani, M.-A.; Espinosa-Gomez, A.; Ngov, K.; White, J.; Buscher, T.; Separovic, F.; O'Mara, M. L.; Coote, M. L.; Connal, L. A. A multifunctional surfactant catalyst inspired by hydrolases. *Sci. Adv.* **2020**, *6*, No. eaaz0404. (b) Hu, L.; Zhao, Y. Cross-Linked Micelles with Enzyme-like Active Sites for Biomimetic Hydrolysis of Activated Esters. *Helv. Chim. Acta* **2017**, *100*, No. e1700147. (c) Tonellato, U. Functional Micellar Catalysis. Part 2. Ester Hydrolysis Promoted by Micelles Containing the Imidazole Ring and the Hydroxy-Group. *J. Chem. Soc., Perkin Trans. 2* **1977**, *6*, 821–827.
- (15) Nothling, M. D.; Xiao, Z.; Bhaskaran, A.; Blyth, M. T.; Bennett, C.; Coote, M. L.; Connal, L. A. Synthetic Catalysts Inspired by Hydrolytic Enzymes. *ACS Catal.* **2019**, *9*, 168–187.
- (16) (a) Oinonen, C.; Ruovinen, J. Structural comparison of Ntn-hydrolases. *Protein Sci.* **2000**, *9*, 2329–2337. (b) Zhiryakova, D.; Ivanov, I.; Ilieva, S.; Guncheva, M.; Galunsky, B.; Stambolieva, N. Do N-terminal nucleophile hydrolases indeed have a single amino acid catalytic center? Supporting amino acid residues at the active site of penicillin G acylase. *FEBS J.* **2009**, *276*, 2589–2598. (c) Ekici, O. D.; Paetzel, M.; Dalbey, R. E. Unconventional serine proteases: Variations



on the catalytic Ser/His/Asp triad configuration. *Protein Sci.* **2008**, *17*, 2023–2037. (d) Oinonen, C.; Tikkanen, R.; Rouvinen, J.; Peltonen, L. Three-dimensional structure of human lysosomal aspartylglucosaminidase. *Nat. Struct. Mol. Biol.* **1995**, *2*, 1102–1108.

(17) (a) Brannigan, J. A.; Dodson, G.; Duggleby, H. J.; Moody, P. C. E.; Smith, J. L.; Tomchick, D. R.; Murzin, A. G. A protein catalytic framework with an N-terminal nucleophile capable of self-activation. *Nature* **1995**, *378*, 416–419. (b) Oinonen, C.; Rouvinen, J. *Protein Sci.* **2000**, *9*, 2329–2337.

(18) (a) Lee, Y. S.; Kim, H. W.; Park, S. S. The Role of  $\alpha$ -Amino Group of the N-terminal Serine of  $\alpha$ -Subunit for Enzyme Catalysis and Autoproteolytic Activation of Glutaryl 7-Aminocephalosporanic Acid Acylase. *J. Biol. Chem.* **2000**, *275*, 39200–39206. (b) Morillas, M.; Goble, M. L.; Virden, R. The kinetics of acylation and deacylation of penicillin acylase from *Escherichia coli* ATCC 11105: evidence for lowered  $pK_a$  values of groups near the catalytic centre. *Biochem. J.* **1999**, *338*, 235–239.

(19) Kirby, A. J.; Hollfelder, F. *From Enzyme Models to Model Enzymes*; RSC Publishing: Cambridge, U.K., 2009; p 4.

(20) Schutz, C. N.; Warshel, A. The low barrier hydrogen bond (LBHB) proposal revisited: The case of the Asp ... His pair in serine proteases. *Proteins: Struct., Funct., Genet.* **2004**, *55*, 711–723.

(21) Hedstrom, L. Serine Protease Mechanism and Specificity. *Chem. Rev.* **2002**, *102*, 4501–4523.

(22) Chen, H.; Weiner, W. S.; Hamilton, A. D. Recognition of neutral species with synthetic receptors. *Curr. Opin. Chem. Biol.* **1997**, *1*, 458–466.

(23) Wayman, K. A.; Sammakia, T. O-Nucleophilic Amino Alcohol Acyl-Transfer Catalysts: The Effect of Acidity of the Hydroxyl Group on the Activity of the Catalyst. *Org. Lett.* **2003**, *5*, 4105–4108.

(24) (a) D'Souza, V. T.; Bender, M. L. Miniature organic models of enzymes. *Acc. Chem. Res.* **1987**, *20*, 146–152. (b) Breslow, R.; Nesnas, N. Burst kinetics and turnover in an esterase mimic. *Tetrahedron Lett.* **1999**, *40*, 3335–3338. (c) Fersht, A. *Structure and Mechanism in Protein Science, A Guide to Enzyme Catalysis and Protein Folding*, 2nd ed.; W. H. Freeman: New York, 1999; pp 218–231.

(25) Menger, F. M.; Whitesell, L. G. A protease mimic with turnover capabilities. *J. Am. Chem. Soc.* **1985**, *107*, 707–708.

(26) Estevan, C.; Vilanova, E. Ethyl Acetate. In *Encyclopedia of Toxicology*, 3rd ed.; Academic Press: London, 2014; pp 506–510.

(27) Breslow, R. Biomimetic Chemistry and Artificial Enzymes: Catalysis by Design. *Acc. Chem. Res.* **1995**, *28*, 146–153.

(28) Duggleby, H. J.; Tolley, S. P.; Hill, C. P.; Dodson, E. J.; Dodson, G.; Moody, P. C. E. Penicillin acylase has a single-amino-acid catalytic centre. *Nature* **1995**, *373*, 264–268.

(29) Marlin, D. S.; Olmstead, M. M.; Mascharak, P. K. Extended structures controlled by intramolecular and intermolecular hydrogen bonding: a case study with pyridine-2,6-dicarboxamide, 1,3-benzenedicarboxamide and *N,N'*-dimethyl-2,6-pyridinedicarboxamide. *J. Mol. Struct.* **2000**, *554*, 211–223.

(30) (a) Simón, L.; Goodman, J. M. Enzyme Catalysis by Hydrogen Bonds: The Balance between Transition State Binding and Substrate Binding in Oxyanion Holes. *J. Org. Chem.* **2010**, *75*, 1831–1840. (b) Simón, L.; Goodman, J. M. Hydrogen-bond stabilization in oxyanion holes: *grand jeté* to three dimensions. *Org. Biomol. Chem.* **2012**, *10*, 1905–1913.